Liquid ternary aerosols of $HNO_3/H_2SO_4/H_2O$ in the Arctic tropopause region

H. Irie,[1] Y. Kondo,[2] M. Koike,[3] N. Takegawa,[2] A. Tabazadeh,[4] J. M. Reeves,[5]
G. W. Sachse,[6] S. A. Vay,[6] B. E. Anderson,[6] and M. J. Mahoney[7]

[1] Measurements of total reactive nitrogen (NO_y) concentrations in the gas and aerosol phases were made on board the NASA DC-8 aircraft within 1 km above the Arctic tropopause in February 2000. As temperatures decreased, NO_y was taken up into the background sulfate aerosols. The observed temperature-dependent NO_y uptake agrees well with that calculated from a model of nitric acid (HNO_3) uptake to form liquid $HNO_3/H_2O/H_2SO_4$ ternary droplets. The observations reported here provide the first direct evidence for the formation of ternary droplets in the Arctic tropopause region. *INDEX TERMS:* 0305 Atmospheric Composition and Structure: Aerosols and particles (0345, 4801); 0320 Atmospheric Composition and Structure: Cloud physics and chemistry; 0340 Atmospheric Composition and Structure: Middle atmosphere—composition and chemistry. **Citation:** Irie, H., Y. Kondo, M. Koike, N. Takegawa, A. Tabazadeh, J. M. Reeves, G. W. Sachse, S. A. Vay, B. E. Anderson, and M. J. Mahoney (2004), Liquid ternary aerosols of $HNO_3/H_2SO_4/H_2O$ in the Arctic tropopause region, *Geophys. Res. Lett.*, *31*, L01105, doi:10.1029/2003GL018678.

1. Introduction

[2] In the tropopause region, cirrus clouds play an important role in Earth's radiation budget through not only scattering and absorbing radiation [*Liou*, 1986], but also altering the partitioning of reactive nitrogen (NO_y) [*Kondo et al.*, 2003]. NO_y plays an important role in controlling the budget of ozone near the tropopause. The ozone near the tropopause is known as the third most important greenhouse gas after water vapor and carbon dioxide [*IPCC*, 2001]. Cirrus cloud radiative impacts are primarily controlled by the number concentration, size, and shape of the ice crystals in the clouds, and properties that are closely linked to mechanisms by which cloud particles nucleate and grow in the atmosphere. Thus far, the homogeneous freezing of sulfate aerosol particles has been identified as an important process in ice particle nucleation in the tropopause region

[e.g., *Jensen et al.*, 1998, 2001]. Recently, it was predicted by a model that the sulfate aerosols incorporate a significant amount of nitric acid (HNO_3) to form liquid ternary aerosols (LTA) of $HNO_3/H_2SO_4/H_2O$ in the tropopause region [*Lin and Tabazadeh*, 2001]. Since the LTA particles have a larger volume and surface area than those of sulfate aerosols, ice crystal formation through homogeneous freezing of LTA may take place more effectively. Furthermore, the homogeneous freezing of LTA may lead to the formation of nitric acid trihydrate (NAT) as in the polar stratosphere [*Tabazadeh et al.*, 2002; *Irie and Kondo*, 2003], altering tropopause aerosol characteristics. Prior to this work, however, there has been no direct evidence for LTA formation in the tropopause region.

[3] The SAGE III Ozone Loss and Validation Experiment (SOLVE) was conducted near Kiruna, Sweden (67°N, 21°E), from December 1999 to March 2000. During SOLVE, measurements of NO_y in both gas and aerosol phases were made simultaneously on board the NASA DC-8 aircraft in the Arctic upper troposphere and lowermost stratosphere. In this paper, we focus on the DC-8 flight starting on February 27 and ending on February 28, 2000. These measurements are used to provide evidence for the uptake of NO_y to form LTA droplets in the tropopause region.

2. Aircraft Measurements

[4] During the SOLVE campaign, NO_y was measured by a chemiluminescence technique combined with a heated gold catalytic converter on board the NASA DC-8 aircraft [*Koike et al.*, 2002; *Kondo et al.*, 2003]. Two independent inlets (with an inner diameter of 6.38 mm and a mass flow rate of 0.94 slm) were placed over the right wing of the DC-8, one directed forward and the other rearward. Both inlets were heated to 100°C to evaporate particles during the sampling. Particulate NO_y was released during the evaporation and was subsequently converted to NO by the gold catalyst.

[5] In the absence of NO_y-containing aerosols, the NO_y signal obtained from the forward inlet (FNO_y) is identical to the rear NO_y signal (RNO_y). On the other hand, when NO_y-containing aerosols are encountered, the FNO_y signal differs from RNO_y due to the anisokinetic sampling of the particles. The two signals are related to the amounts of NO_y in the gas phase (NO_y^g) and the condensed phase (NO_y^c) as follows:

$$FNO_y = NO_y^g + EF \times NO_y^c \qquad (1)$$

$$RNO_y = NO_y^g + \alpha \times NO_y^c \qquad (2)$$

---

[1]National Institute for Environmental Studies, Tsukuba, Ibaraki, Japan.
[2]Research Center for Advanced Science and Technology, University of Tokyo, Meguro, Tokyo, Japan.
[3]Department of Earth and Planetary Science, Graduate School of Science, University of Tokyo, Tokyo, Japan.
[4]NASA Ames Research Center, Moffett Field, California, USA.
[5]Department of Engineering, University of Denver, Denver, Colorado, USA.
[6]NASA Langley Research Center, Hampton, Virginia, USA.
[7]Jet Propulsion Laboratory, California Institute of Technology, Pasadena, California, USA.

where EF and α are enhancement and reduction factors of NO_y^c, respectively. While air streamlines rapidly diverge as they approach the forward-facing inlet, particles with sufficient inertia cross the streamlines, enhancing the amount of NO_y^c (i.e., $EF \geq 1$). For the rearward-facing inlet, only small particles can change their flow directions, due to their small inertia, and enter the inlet, reducing the amount of NO_y^c (i.e., $0 \leq \alpha \leq 1$). The values of EF and α are primarily a function of the size distribution and the density of aerosols, the ambient pressure, and the DC-8 cruise speed. Although NO_y^c should be estimated using EF and α functions of our instrument, because of a lack of these functions, this study estimates the NO_y^c from the measured FNO_y and RNO_y signals and an empirical function of EF, as described below.

[6] Dry aerosol size distributions for diameters up to ~ 2 μm were obtained by an inversion of size distributions measured by the Focused Cavity Aerosol Spectrometer (FCAS) II [*Jonsson et al.*, 1995] and Nuclei-Mode Aerosol Size Spectrometer (N-MASS) [*Brock et al.*, 2000]. Using the equilibrium density of the particles of H_2SO_4/H_2O and acid mass fraction, the aerosol size was corrected for water evaporation during the sampling to be $57 \pm 3\%$ larger than those observed for the period analyzed in this study. Since no correction technique has been established for the evaporation of HNO_3 during the sampling, the size of aerosols could be underestimated when HNO_3 was condensed in ambient aerosols. Aerosol size distributions for diameters of $0.4-20$ μm were measured by the Forward Scattering Spectrometer Probe (FSSP)-300. Water vapor (H_2O) and nitrous oxide (N_2O) mixing ratios were measured with the near-IR tunable Diode Laser Hygrometer (DLH) [*Vay et al.*, 2000, and references therein] and a folded-path differential absorption mid-IR diode laser spectrometer (DACOM) [*Sachse et al.*, 1991], respectively. The tropopause height was calculated from temperature profiles observed by the Microwave Temperature Profiler (MTP) instrument [*Denning et al.*, 1989] on board DC-8.

3. Estimate of NO_y Condensed in Aerosols

[7] We used two different techniques to estimate NO_y^c from the measured signals of FNO_y and RNO_y. First, we used the difference between FNO_y and RNO_y. From this difference and equations 1 and 2, the NO_y^c can be expressed as:

$$\left(FNO_y - RNO_y\right)/(EF - \alpha) \tag{3}$$

As particles grow taking up NO_y, the EF increases and α decreases, resulting in an increase in the value of $FNO_y - RNO_y$. Thus, the difference between the FNO_y and RNO_y signals represents the relative change in the amount of NO_y condensed in aerosols. Second, we used the difference between NO_y^* and RNO_y. Here NO_y^* is the concentration of the unperturbed NO_y (corresponding to the gas-phase NO_y in an air mass without the uptake of NO_y into particles), which was derived from the DACOM N_2O data and $NO_y - N_2O$ correlations obtained over the Arctic in February and March 2000 [*Koike et al.*, 2002]. The NO_y^* was systematically smaller than RNO_y by ~ 50 pptv just before and after the DC-8 encountered NO_y-containing aerosols on

February 28, 2000 (not shown). However, this difference is smaller than the standard deviation of NO_y mixing ratios (~ 150 ppbv) obtained near the Arctic tropopause ($N_2O = 310 \pm 5$ ppbv), so that the difference likely resulted from natural inhomogeneity of NO_y (e.g., nitrification [*Koike et al.*, 2002]) over the Arctic region from February to March 2000. Therefore, the NO_y^* used in this study was increased by 50 pptv to agree with RNO_y in the absence of NO_y-containing aerosols. Thereby, we can assume that the amount of NO_y condensed in aerosols is equal to the gas-phase reduction in NO_y:

$$NO_y^c = NO_y^* - NO_y^g \tag{4}$$

Using this and equation 2, NO_y^c can be expressed as:

$$\left(NO_y^* - RNO_y\right)/(1 - \alpha) \tag{5}$$

The value of $1 - \alpha$ is less than 1 so that the difference between NO_y^* and RNO_y is interpreted as a lower limit of NO_y^c.

4. Model Calculation

[8] We used a thermodynamic equilibrium model for the $HNO_3/H_2SO_4/H_2O$ system (LTA model) [*Lin and Tabazadeh*, 2001] to calculate the amount of HNO_3 condensed in aerosols. The total (gas + condensed phases) HNO_3 concentration used in the model calculation was derived from $NO_y^* \times 0.9$ (an average of HNO_3/NO_y ratios in the Arctic tropopause region [*Ballenthin et al.*, 2003]). The total H_2O concentration was taken from the DLH H_2O measurements. We derived the H_2SO_4 loading from the size distributions measured by FCAS-II and N-MASS assuming thermodynamic equilibrium.

5. Results and Discussion

[9] During $4.0-5.0$ UT hours on February 28, 2000, the DC-8 aircraft cruised with a speed of 220 m sec^{-1} at an altitude of 11.3 km (~ 220 hPa) over the eastern coast of Greenland ($77°-78°N$ and $40°-10°W$). Temperature profiles obtained from MTP indicated that the DC-8 was at $0-1.3$ km above the tropopause (Figure 1a). The jumps in the tropopause height in Figure 1a are due to the complicated temperature structure associated with a stratospheric intrusion near the edge of the vortex. The H_2O mixing ratios ranged between 8 and 11 ppmv (Figure 1b). The N_2O mixing ratios varied slightly from 305 to 312 ppbv (not shown), suggesting that the background states (size distribution and number concentration) of aerosols were similar for air masses observed throughout this period [*Drdla et al.*, 2003]. The sampled air masses cooled to $201-206$ K (Figure 1c). In particular, at 4.4 hours, the temperature dropped to below the saturation temperature for nitric acid trihydrate ($T_{NAT} \sim 204$ K) [*Hanson and Mauersberger*, 1988]. Near 20 km, NO_y-containing particles (LTA and NAT) were measured at temperatures below T_{NAT} (~ 195 K) over the Arctic during SOLVE [*Drdla et al.*, 2003; *Fahey et al.*, 2001].
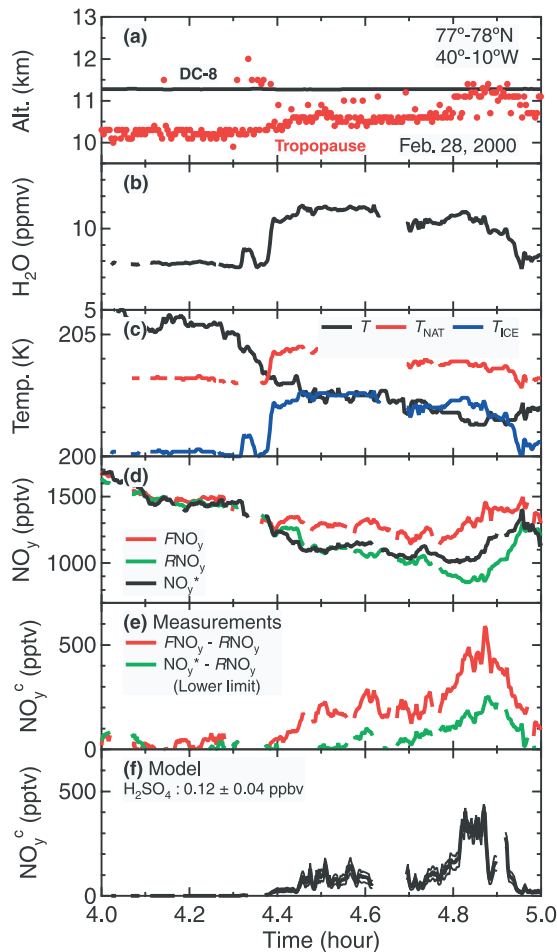
Figure 1. Time series plots of parameters obtained at $77°-78°N$, and $40°-10°W$ at $4.0-5.0$ UT hours on February 28, 2000: (a) DC-8 flight altitude (black) and tropopause height obtained from MTP data (red), (b) H_2O mixing ratio, (c) ambient temperature and saturation points for NAT (T_{NAT}) and ice (T_{ICE}), (d) measured signals of FNO_y (red) and RNO_y (green) and calculated unperturbed NO_y (NO_y^*) (black), (e) difference between FNO_y and RNO_y (red) and the difference between NO_y^* and RNO_y (green), and (f) condensed-phase NO_y calculated from a liquid ternary aerosol model. The value of $NO_y^* - RNO_y$ is interpreted as a lower limit of condensed NO_y^c as discussed in the text.

[10] At $4.4-4.9$ hours, a departure of FNO_y from RNO_y was observed (Figures 1d and 1e), indicating that a significant amount of NO_y was condensed into the aerosol phase. We also detected the loss of gas-phase NO_y as a difference between NO_y^* and RNO_y (Figures 1d and 1e). The difference between NO_y^* and RNO_y is interpreted as a lower-limit estimate of NO_y^c, as described above.

[11] NO_y^c is quantified also from the difference between FNO_y and RNO_y, when EF is estimated. The EF was estimated by comparing the value of $FNO_y - RNO_y$ with the lower limit of NO_y^c (defined as $NO_y^* - RNO_y$). For $4.5-4.7$ hours and $4.8-4.9$ hours, the values of $FNO_y - RNO_y$ are ~200 and ~450 pptv, respectively, where the lower limits are ~50 and ~150 pptv (Figure 1e). Since
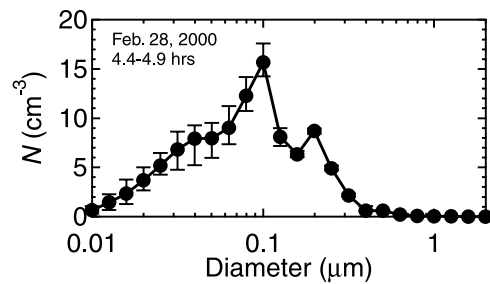
Figure 2. Median size distribution of number concentrations in each size bin at $4.4-4.9$ hours on February 28, 2000. Error bars represent the 67% ranges.

$FNO_y - RNO_y$ divided by $EF - \alpha$ must be equal to or greater than the lower limit as defined in equation 3 and α must range from 0 to 1, the EF was estimated to be 4 ± 1 or smaller. Using an empirical expression [*Durham and Lundgren*, 1980], a particle density of 1.3 g cm^{-3} (obtained from the LTA model), and the measured size distribution up to 2 μm by FCAS-II and N-MASS (Figure 2), the EF was also estimated to be ~20 (Figure 3). This value was much greater than the EF estimated from the NO_y measurements.

[12] The NO_y probe was placed over the right wing of the DC-8, such that it was possible that the ambient pressure diminished to ~180 hPa, based on the local flow investigations made at the NO_y probe location after the SOLVE campaign. However, the reduction in the pressure has a much smaller influence on estimating EF, as compared to the difference with EF estimated from NO_y measurements (Figure 3).

[13] Causes leading to the discrepancy in EFs obtained from the NO_y measurements and the empirical equation are currently unknown. One of the possible causes is that the empirical equation for the EF calculation by *Durham and Lundgren* [1980] cannot be applied to the NO_y instrument used in this study. Or, a change in aerosol distributions might occur near the NO_y inlet probe, which was placed over the wing of the DC-8. Another explanation is that the uptake of NO_y might be confined to the small particles due to the rapid temperature fluctuation caused by lee waves [*Meilinger et al.*, 1995]. If NO_y were condensed only into particles smaller than 0.11 ± 0.04 μm, the EF would drop to
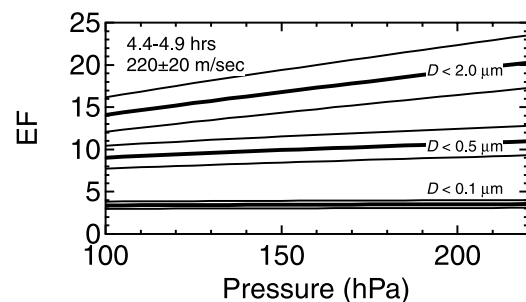
Figure 3. Enhancement factor (EF) as a function of ambient pressure for FNO_y measurements at a DC-8 cruise speed of 220 m sec^{-1} (thick lines). EFs are shown for aerosol size distributions up to 2.0, 0.5, and 0.1 μm. For reference, calculations for DC-8 cruise speeds of 200 and 240 m sec^{-1} are also shown (thin lines).
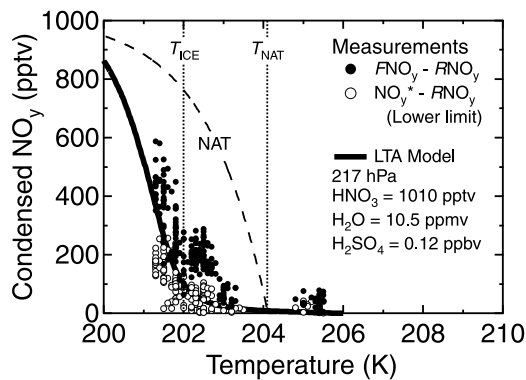
Figure 4. Temperature dependence of NO_y condensed in aerosols obtained from measurements (circles) and a liquid ternary aerosol model (lines). For reference, the equilibrium curve for NAT formation is shown with the dashed line.

4 ± 1 (Figure 3). To address this issue, further analyses and observations are needed.

[14] As seen in Figure 1e, the uptake of NO_y into aerosols started at 4.4 hours and increased between 4.4 and 4.9 hours during the DC-8 flight on February 28, 2000. This increase in NO_y^c occurred as temperatures dropped from 204 K to 201 K (Figure 4). As shown by *Kondo et al.* [2003], at 200–215 K significant adsorption of NO_y on ice crystal surfaces was observed at altitudes of 8–12 km over the Arctic when the total surface area density (SA) was ≈ 10–$1000 \ \mu m^2 cm^{-3}$ for particles (with diameters of 0.4–20 μm) measured by FSSP. At 4.4–4.9 hours on February 28, 2000, however, the total SA measured by FSSP was smaller than $1 \ \mu m^2 cm^{-3}$, indicating very limited or no NO_y adsorption on ice crystals. Instead, these results suggest the LTA formation through the condensation of HNO_3 into sulfate aerosols at cold temperatures. To quantitatively evaluate the LTA formation, we calculated the amount of the HNO_3 uptake by using an LTA model, total HNO_3 = 1010 pptv, total H_2O = 10.5 ppmv (mean values at 4.4–4.9 hours), and total H_2SO_4 = 0.12 ppbv (derived from FCAS and N-MASS data at 4.4–4.9 hours) (Figures 1f and 4). From the uncertainty of the aerosol total volume measurements by FCAS and N-MASS, the uncertainty of H_2SO_4 was estimated to be as small as 0.04 ppbv. As seen in these figures, the model also predicted LTA formation by the condensation of HNO_3 starting at 204 K and increasing to ~400 pptv at 201 K. Therefore, we conclude that the NO_y-containing particles measured in the Arctic tropopause region were made of LTA. LTA particles freeze into ice crystals more effectively than sulfate aerosols because of a larger volume and surface area, and thus the LTA formation process should be considered in model simulations of aerosols and clouds in the tropopause region.

6. Conclusions

[15] We measured concentrations of NO_y condensed in aerosols to investigate the aerosol chemical composition in the Arctic tropopause region. Within 1 km above the tropopause, the uptake of NO_y into aerosols was observed starting at 204 K and increasing between 204 and 201 K. The temperature dependence of the measured NO_y uptake

was well reproduced by a box model for ternary droplets of $HNO_3/H_2SO_4/H_2O$, indicating the presence of ternary droplets in the Arctic tropopause region. Our results suggest that cirrus ice formation near the Arctic tropopause may sometimes occur through homogeneous freezing of LTA droplets.

References

Ballentin, J. O., W. F. Thorn, T. M. Miller, A. A. Viggiano, D. E. Hunton, M. Koike, Y. Kondo, N. Takegawa, H. Irie, and H. Ikeda (2003), In situ HNO_3 to NO_y instrument comparison during SOLVE, *J. Geophys. Res.*, 108(D6), 4188, doi:10.1029/2002JD002136.

Brock, C. A., F. Schröder, B. Kärcher, A. Petzold, R. Busen, and M. Fiebig (2000), Ultrafine particle size distributions measured in aircraft exhaust plumes, *J. Geophys. Res.*, 105(D21), 26,555–26,567.

Denning, R. F., S. L. Guidero, G. S. Parks, and B. L. Gary (1989), Instrument description of the airborne microwave temperature profiler, *J. Geophys. Res.*, 94(D14), 16,757–16,765.

Drdla, K., B. W. Gandrud, D. Baumgardner, J. C. Wilson, T. P. Bui, D. Hurst, S. M. Schauffler, H. Jost, J. B. Greenblatt, and C. R. Webster (2003), Evidence for the widespread presence of liquid-phase particles during the 1999–2000 Arctic winter, *J. Geophys. Res.*, 108(D5), 8318, doi:10.1029/2001JD001127.

Durham, M. D., and D. A. Lundgren (1980), Evaluation of aerosol aspiration efficiency as a function of Stokes number, velocity ratio and nozzle angle, *J. Aerosol Sci.*, 11, 179–188.

Fahey, D. W., et al. (2001), The detection of large HNO_3-containing particles in the winter Arctic stratosphere, *Science*, 291, 1026–1031.

Hanson, D., and K. Mauersberger (1988), Laboratory studies of the nitric acid trihydrate: Implications for the south polar stratosphere, *Geophys. Res. Lett.*, 15(8), 855–858.

Intergovernmental Panel on Climate Change (IPCC) (2001), *Third Assessment Report*, Cambridge Univ. Press, New York.

Irie, H., and Y. Kondo (2003), Evidence for the nucleation of polar stratospheric clouds inside liquid particles, *Geophys. Res. Lett.*, 30(4), 1189, doi:10.1029/2002GL016493.

Jensen, E. J., et al. (1998), Ice nucleation processes in upper tropospheric wave-clouds observed during SUCCESS, *Geophys. Res. Lett.*, 25(9), 1363–1366.

Jensen, E. J., O. B. Toon, S. A. Vay, J. Ovarlez, R. May, T. P. Bui, C. H. Twohy, B. W. Gandrud, R. F. Pueschel, and U. Schumann (2001), Prevalence of ice-supersaturated regions in the upper troposphere: Implications for optically thin ice cloud formation, *J. Geophys. Res.*, 106(D15), 17,253–17,266.

Jonsson, H. H., et al. (1995), Performance of a focused cavity aerosol spectrometer for measurements in the stratosphere of particle size in the 0.06–2.0 μm diameter range, *J. Atmos. Oceanic Technol.*, 12, 115–129.

Koike, M., et al. (2002), Redistribution of reactive nitrogen in the Arctic lower stratosphere in the 1999/2000 winter, *J. Geophys. Res.*, 107(D20), 8275, doi:10.1029/2001JD001089.

Kondo, Y., et al. (2003), Uptake of reactive nitrogen on cirrus cloud particles in the upper troposphere and lowermost stratosphere, *Geophys. Res. Lett.*, 30(4), 1154, doi:10.1029/2002GL016539.

Lin, J.-S., and A. Tabazadeh (2001), A parameterization of an aerosol physical chemistry model for the $NH_3/H_2SO_4/HNO_3/H_2O$ system at cold temperatures, *J. Geophys. Res.*, 106(D5), 4815–4829.

Liou, K. N. (1986), Influence of cirrus clouds on weather and climate processes: A global perspective, *Mon. Wea. Rev.*, 114, 1167–1199.

Meilinger, S. K., T. Koop, B. P. Luo, T. Huthwelker, K. S. Carslaw, U. Krieger, P. J. Crutzen, and Th. Peter (1995), Size-dependent stratospheric droplet composition in lee wave temperature fluctuations and their potential role in PSC freezing, *Geophys. Res. Lett.*, 22(22), 3031–3034.

Sachse, G. W., J. E. Collins, G. F. Hill, L. O. Wade, L. G. Burney, and J. A. Ritter (1991), Airborne tunable diode laser system for high precision concentration and flux measurements of carbon monoxide and methane, *SPIE Proceedings*, 1433, 145–156.

Tabazadeh, A., Y. S. Djikaev, P. Hamill, and H. Reiss (2002), Laboratory evidence for surface nucleation of solid polar stratospheric cloud particles, *J. Phys. Chem. A*, 106, 10,238–10,246.

Vay, S. A., B. E. Anderson, E. J. Jensen, G. W. Sachse, J. Ovarlez, G. L. Gregory, S. R. Nolf, J. R. Podolske, T. A. Slate, and C. E. Sorenson (2000), Tropospheric water vapor measurements over the North Atlantic during the Subsonic Assessment Ozone and Nitrogen Oxide Experiment (SONEX), *J. Geophys. Res.*, *105*(D3), 3745–3755.

————————————

B. E. Anderson, G. W. Sachse, and S. A. Vay, NASA Langley Research Center, Hampton, VA 23681-2199, USA.

H. Irie, National Institute for Environmental Studies, Satellite Remote Sensing Research Team, 16-2, Onogawa, Tsukuba, Ibaraki 305-8506, Japan. (irie.hitoshi@nies.go.jp)

M. Koike, Department of Earth and Planetary Science, Graduate School of Science, University of Tokyo, Bunkyo, Tokyo 113-0033, Japan.

Y. Kondo and N. Takegawa, Research Center for Advanced Science and Technology, University of Tokyo, 4-6-1, Komaba, Meguro, Tokyo 153-8904, Japan.

M. J. Mahoney, Jet Propulsion Laboratory, California Institute of Technology, MS 246-102, 4800 Oak Grove Drive, Pasadena, CA 91109-8099, USA.

J. M. Reeves, Department of Engineering, University of Denver, Denver, CO 80208-0177, USA.

A. Tabazadeh, NASA Ames Research Center, MS 245-4, Moffett Field, CA 94035-1000, USA.